Nonstationary Atmospheric Boundary-Layer Turbulence Simulation

George H. Fichtl*
NASA Marshall Space Flight Center, Ala.
and
Morris Perlmutter†
Northrop Services, Inc., Huntsville, Ala.

The vertical nonhomogeneous character of turbulence in the atmospheric boundary layer results in a nonstationary turbulence process relative to an aircraft during takeoff and landing despite the fact that the turbulence statistics can be horizontally homogeneous. The simulation of this nonstationary aspect of atmospheric turbulence is the subject of this paper. A procedure is developed and demonstrated with a longitudinal component of turbulence random process field $u(x,z)$, where x and z denote horizontal and vertical coordinates, which has Dryden autospectra with integral scale L that depends linearly on height above natural grade and two-point statistics (interlevel cross-correlations) which obey Davenport-Panofsky scaling laws. It is shown that for these assumed properties of the turbulent field that the random process field $v(x,z)$ which possesses first- and second-moment statistics equal to those of $u(x,z)$ can be transformed to the random function $v(x,z)/\sigma(z)L^{1/2}(z)=F(x/z)$ where $\sigma(z)$ is the standard deviation at height z of the random process $u(x,z)$, and $F(x/z)$ is a random function of x/z. The above stated transformation property and Taylor's frozen eddy hypothesis permits the generation of the process $F(x/z)$ with white noise from which the random process $v(t)=v(X(t), Z(t))$ along the aircraft trajectory $(X(t), Z(t)$, can be used as a simulation of the random process $u(t)=u(X(t), Z(t))$.

I. Introduction

ATMOSPHERIC turbulence has plagued manned powered flight since the first flight of the Wright Brothers at Kitty Hawk, North Carolina in 1903.[1] During the years that followed that pioneering event an ever increasing number of studies have been devoted to the problem of designing aircraft control systems and structures capable of negotiating and withstanding the vicious attacks of atmospheric turbulence. This has been especially true during the last ten years relative to the design of automatic landing control systems for both aircraft[2] and aerospace vehicles like the forthcoming Space Shuttle.[3] To evaluate a control system design, it is common practice to simulate flight in turbulence on computers with turbulence-like random processes generated by filtering random noise processes such that the second-moment statistics of the generated random process resemble those obtained in atmospheric turbulence. Many techniques have been used to simulate atmospheric turbulence.[4] The majority of these techniques are based on the Dryden hypothesis of the Eulerian spectral density function of the turbulence[5] and Taylor's frozen eddy hypothesis.[6] A major criticism of the existing engineering turbulence simulation schemes for the atmospheric boundary layer is that they fail to account for the statistically nonhomogeneous character of atmospheric boundary-layer turbulence along the vertical. It is this nonhomogeneous feature which results in the turbulence appearing as a nonstationary process relative to an aircraft during takeoff and landing.

Presented as Paper 74-587 at the AIAA 7th Fluid and Plasma Dynamics Conference, Palo Alto California, June 17-19, 1974; submitted July 15, 1974; revision received December 23, 1974. The authors acknowledge J. Enders of the Aeronautical Operating Systems Office, Office of Aeronautics and Space Technology, NASA, Washington, D.C., for the support he provided to accomplish the research reported herein.

Index categories: Aircraft Gust Loading and Wind Shear; Aircraft Handling, Stability, and Control; Aircraft Landing Dynamics.

*Chief, Environmental Dynamics Branch. Associate Fellow AIAA.

†Aerospace Engineer. Presently at the University of Tennessee Space Institute, Tullahoma, Tennessee.

It is the goal of this paper to report new and general techniques for simulating atmospheric turbulence-like random processes which are statistically homogeneous along the horizontal and nonhomogeneous along the vertical. This technique is general in the sense that it can be used for a broad class of similar problems. Like the other presently available schemes the techniques presented herein are based on the Dryden hypothesis and Taylor's frozen eddy hypothesis; however, our technique goes a step further by utilizing certain self-similarity properties of the Dryden spectral density function which permits the development of height invariant filters. These filters are in turn used to generate vertically homogeneous (statistically) random processes from which turbulence at any specified level in the boundary layer can be simulated; thus, facilitating the simulation of a nonstationary turbulence process along the flight path of an aircraft during takeoff or landing.

II. Definition of Problem

A one-dimensional Fourier decomposition of the longitudinal component of turbulence $u(x,y,z,t)$ along the x-axis (directed along the mean wind vector) in a coordinate system moving with the mean wind is given by

$$u(x,y,z,t)=\int_{-\infty}^{\infty}\hat{u}(\kappa,y,z,t)e^{i\kappa x}\mathrm{d}\kappa \tag{1}$$

where $\hat{u}(\kappa,y,z,t)$ is the Fourier transform of $u(x,y,z,t)$ at wave number $\kappa(\text{rad m}^{-1})$. The y- and z-axes are orthogonal to the x-axis with the z-axis directed along the upward vertical. In the discussion that follows we will be concerned with the simulation of turbulence fields in the (x,z)-plane at a given instant, so that we shall not carry y and t along in the analysis. Although the discussion is confined to the longitudinal component of turbulence the analysis is sufficiently general so as to be applicable to the simulation of the lateral and vertical components of turbulence.

Let us now construct the longitudinal correlation function by evaluating Eq. (1) at (x,z) and its complex conjugate at

$(x+r, z-\Delta)$, multiplying the resulting relationships, and then averaging over the ensemble of products to obtain

$$R(r,\Delta,x,z) = \langle u(x,z)\ u(x+r,z-\Delta)\rangle$$

$$= \int_{-\infty}^{\infty}\int_{-\infty}^{\infty} \langle \hat{u}(\kappa,z)\hat{u}^*(\kappa',z-\Delta)\rangle e^{i(\kappa-\kappa')x} e^{-i\kappa' r} d\kappa' d\kappa \quad (2)$$

The analysis that follows shall be restricted to the case of a horizontally homogeneous turbulence process, so that correlation of the Fourier amplitudes must be of the form

$$\langle \hat{u}(\kappa,z)\hat{u}^*(\kappa',z-\Delta)\rangle = \phi(\kappa',\Delta,z)\delta(\kappa'-\kappa) \quad (3)$$

where $\delta(\kappa'-\kappa)$ is the Dirac delta function and $\phi(\kappa',\Delta,z)$ is the interlevel cross-spectral density function. Combination of Eqs. (2) and (3) yields the horizontally homogeneous correlation function

$$R(r,\Delta,z) = \int_{-\infty}^{\infty} \phi(\kappa,\Delta,z) e^{-i\kappa r} d\kappa \quad (4)$$

We now express the interlevel cross-spectral density function $\phi(\kappa,\Delta,z)$ in terms of the spectral coherence and phase angle, namely

$$\text{Coh}\ (\kappa,\Delta,z) = \frac{\phi(\kappa,\Delta,z)\ \phi^*(\kappa,\Delta,z)}{\phi(\kappa,o,z)\ \phi(\kappa,o,z-\Delta)} \quad (5)$$

$$\theta(\kappa,\Delta,z) = \tan^{-1}\left[\frac{Im[\phi(\kappa,\Delta,z)]}{Re[\phi(\kappa,\Delta,z)]}\right] \quad (6)$$

so that

$$\phi(\kappa,\Delta,z) = [\phi(\kappa,o,z)\ \phi(\kappa,o,z-\Delta)\,\text{Coh}(\kappa,\Delta,z)]^{1/2} \times e^{-i\theta(\kappa,\Delta,z)} \quad (7)$$

where $\phi(\kappa,o,z)$ is the auto-spectral density function. Thus, specification of functions $\phi(\kappa,o,z)$, coh (κ,Δ,z) and $\theta(\kappa,\Delta,z)$ serves to completely specify the function $\phi(\kappa,\Delta,z)$ and hence the second-moment statistics of $u(x,z)$ in view of Eq. (4). In the development that follows we seek a filter such that upon input of white noise processes an output process $v(x,z)$ which possesses second moment statistics which resemble those of the process $u(x,z)$ will result. The synthesis of the filter herein is based on the functions $\phi(\kappa,o,z)$, coh (κ,Δ,z) and $\theta(\kappa,\Delta,z)$.

III. Filter Synthesis

The one-dimensional Fourier decomposition of the random process field $v(x,z)$ is given by

$$v(x,z) = \int_{-\infty}^{\infty} \hat{v}(\kappa,z) e^{i\kappa x} d\kappa \quad (8)$$

We begin the simulation of $u(x,z)$ with $v(x,z)$ with n independent horizontally homogeneous Gaussian white noise‡ processes $N_k(x)$ $(k=1,2,\ldots n)$ with the Fourier transform of the kth noise process being $N_k(\kappa)$. We pass the kth noise process through a filter with response function $H_k(\kappa,z)$. A composite process $v_c(x,z)$ is then passed through a linear filter with response function $AH(\kappa,z)$ to obtain the process $v(x,z)$ with Fourier transform

$$\hat{v}(\kappa,z) = AH(\kappa,z)\hat{v}_c(\kappa,z)$$

$$= AH(\kappa,z) \sum_{k=1}^{n} H_k(\kappa,z)\hat{N}_k(\kappa) \quad (9)$$

Multiplication of Eq. (9) by its complex conjugate evaluated at κ' and $z-\Delta$, and ensemble average of the resulting relationship yields

$$\langle \hat{v}(\kappa,z)\hat{v}^*(\kappa',z-\Delta)\rangle = |A|^2 H(\kappa,z)H^*(\kappa',z-\Delta) \times \sum_{k=1}^{n}\sum_{m=1}^{n} \langle \hat{N}_k(\kappa)\hat{N}_m(\kappa')\rangle H_k(\kappa,z)H_m^*(\kappa',z-\Delta) \quad (10)$$

The noise processes are statistically independent and their Fourier transforms are orthogonal with unit spectral density, so that

$$\langle \hat{N}_k(\kappa)\hat{N}_m(\kappa')\rangle = \delta(\kappa-\kappa')\delta_{km} \quad (11)$$

where δ_{km} is Kronecker delta. In view of the fact that we require the second moment statistics of $v(x,z)$ to be identically equal to those of $u(x,z)$ we may write

$$\langle \hat{v}(\kappa,z)\hat{v}(\kappa',z-\Delta)\rangle = \phi(\kappa,\Delta,z)\delta(\kappa-\kappa') \quad (12)$$

so that combination of Eqs. (10-12) yields the cross spectral density function of $u(x,z)$ in terms of the response functions of the components of the filter, i.e.,

$$\phi(\kappa,\Delta,z) = |A|^2 H(\kappa,z)H^*(\kappa,z-\Delta) \times \sum_{k=1}^{n} H_k(\kappa,z)H_k^*(\kappa,z-\Delta) \quad (13)$$

or

$$\phi(\kappa,\Delta,z) = |A|^2 \phi_H(\kappa,\Delta,z)\phi_s(\kappa,\Delta,z) \quad (14)$$

where

$$\phi_H(\kappa,\Delta,z) = H(\kappa,z)H^*(\kappa,z-\Delta) \quad (15a)$$

$$\phi_s(\kappa,\Delta,z) = \sum_{k=1}^{n} H_k(\kappa,z)H_k^*(\kappa,z-\Delta) \quad (15b)$$

A. Coherence Matching

In this section we seek the functions $H_k(\kappa,z)$, $k=1,2,\ldots n$. Substitution of Eq. (13) into Eq. (5) yields the spectral coherence

$$\text{coh}\ (\kappa,\Delta,z) = \frac{\phi_s(\kappa,\Delta,z)\phi_s^*(\kappa,\Delta,z)}{\phi_s(\kappa,o,z)\phi_s^*(\kappa,o,z-\Delta)} \quad (16a)$$

$$= \frac{\sum_{k=1}^{n} H_k(\kappa,z)H_k^*(\kappa,z-\Delta)\ \sum_{m=1}^{n} H_m^*(\kappa,z)H_m(\kappa,z-\Delta)}{\sum_{k=1}^{n} H_k(\kappa,z)H_k^*(\kappa,z)\ \sum_{m=1}^{n} H_m^*(\kappa,z-\Delta)H_m(\kappa,z-\Delta)} \quad (16b)$$

Note that the coherence is independent of $\phi_H(\kappa,\Delta,z)$, as one should expect, so that the function $H(\kappa,z)$ can be reserved for auto-spectra and phase angle matching. Thus, the functions $H_k(\kappa,z)$ will be used to match the filter coherence of $v(x,z)$ with the coherence of $u(x,z)$.

We shall specialize to a class of processes with coherence functions independent of z. The motivation for this specialization results from the fact that the turbulence coherence near the ground ($z \leq 150$ m) appears to behave in this manner. We shall return to this point later.

To formulate a method of satisfying an arbitrary coherence function coh (κ,Δ) we can proceed by assuming that $H_k(\kappa,z)$ is a pure lag, i.e.,

$$H_k(\kappa,z) = C_k e^{-i\kappa z d_k},\ k=1,2,\ldots,n \quad (17)$$

Thus, from Eq. (15b) we obtain

$$\phi_s(\kappa,\Delta) = \sum_{k=1}^{n} C_k^2 e^{-i\kappa d_k \Delta} \quad (18)$$

‡Actually we have in mind a band limited white noise process.

or

$$\mathrm{coh}(\kappa,\Delta) = \frac{\sum_{k=1}^{n} b_k^2 + 2\sum_{m=2}^{n}\sum_{k=1}^{m-1} b_k b_m \cos[(d_m - d_k)\kappa\Delta]}{\sum_{k=1}^{n} b_k^2} \tag{19}$$

where

$$b_k^2 = C_k^2 \tag{20}$$

Examination of the coherence function given by Eq. (19) which is the sum of a finite series of cosine functions suggests that we might determine the b's and d's by expanding the coherence in an even Fourier series on the interval $-\epsilon_o \le \kappa\Delta \le \epsilon_o$, where ϵ_o is the largest value of $\kappa\Delta$ of interest in the simulation. Identification of the coefficients and arguments of the trigometric functions of the said expansion with the corresponding ones in Eq. (19) yields the values of b_k and d_k. The Fourier expansion of the coherence is given by

$$\mathrm{coh}(\xi) = \sum_{j=o}^{\infty} A_j \cos(j\pi\xi) \tag{21}$$

where

$$\xi = \kappa\Delta/\epsilon_o \tag{22}$$

$$A_j = \int_{-1}^{1} \mathrm{coh}(\xi)\cos(j\pi\xi)\,d\xi \tag{23}$$

We now set

$$d_k = \frac{\pi(k-1)}{\epsilon_o} + \beta \tag{24}$$

where β is a constant to be determined through consideration of the phase angle θ. Substitution of Eq. (24) into Eq. (19) and a term by term comparison of Eq. (19) with the first n terms of Eq. (21) yields

$$A_o = \left[1 + \sum_{k=2}^{n} \left(\frac{b_k}{b_1}\right)\right]^{-2}\left[1 + \sum_{k=2}^{n} \left(\frac{b_k}{b_1}\right)^2\right] \tag{25}$$

$$A_j = 2\left[1 + \sum_{k=2}^{n} \left(\frac{b_k}{b_1}\right)\right]^{-2} \times \left[\frac{b_{1+j}}{b_1} + \sum_{k=2}^{n-j} \frac{b_k b_{k+j}}{b_1^2}\right] \tag{26}$$

$$j = 1,2,\ldots n-1$$

We thus have n equations in the n-1 unknowns, b_j/b_1, $j=2,\ldots n$. The quantity b_1 is arbitrary and can be set equal to unity with no loss of generality. A number of methods are available for determining values for the remaining b's. One way is to directly solve the first n-1 equations for b_k, $k=2,\ldots n$. The difficulty with this approach is that for values of $n \ge 4$ the algebraic manipulations involved with determining the solution of the equations become unwieldy. A second approach is to determine a set of values for b_k, $k=2,\ldots n$ which satisfies the n-equations given by Eqs. (25) and (26) subject to the constraint that the positive definite function

$$J = \sum_{j=o}^{n-1} (A_j - A_j')^2 \tag{27}$$

takes on a minimum value, where A_j denotes the coefficients of the Fourier expansion, Eq. (21) and A' denotes the right hand side of Eqs. (25) and (26)

B. Auto-Spectral Density Matching

In this section we seek to determine that part of $H(\kappa,z)$ which is responsible for yielding a turbulence simulation $v(x,z)$ which possesses an assigned functional form for the auto-spectral density function $\phi(\kappa,o,z)$. Evaluation of Eq. (13) at $\Delta = 0$ yields

$$\phi(\kappa,o,z) = |A|^2 \phi_H(\kappa,o,z)\,\phi_s(\kappa,o,z) = |H(\kappa,z)|^2 \tag{28}$$

where we have set

$$|A|^2 = \phi_s^{-1}(\kappa,o,z) = \left[\sum_{k=1}^{n} C_k^2\right]^{-1} \tag{29}$$

Factorization of the left-hand side of Eq. (28) yields $H(\kappa,z)$ to within an arbitrary phase angle. Thus, for example, if $\phi(\kappa,o,z)$ is a meromorphic function then we may write

$$\phi(\kappa,o,z) = B^2 \frac{(1+ia_o\kappa)(1-ia_o\kappa)\ldots(1+ia_\lambda\kappa)(1-ia_\lambda\kappa)}{(1+ib_o\kappa)(1-ib_o\kappa)\ldots(1+ib_\nu\kappa)(1-ib_\nu\kappa)} \tag{30}$$

where λ is not necessarily equal to ν and B is a real positive constant. Factorization of Eq. (30) yields

$$H(\kappa,z) = H_p(\kappa,z)H_\gamma(\kappa,z) \tag{31}$$

where

$$H_p(\kappa,z) = \frac{(1+ia_o\kappa)\ldots(1+ia_\lambda\kappa)}{(1+ib_o\kappa)\ldots(1+ib_\lambda\kappa)} \tag{32}$$

and

$$H_\gamma(\kappa,z) = e^{-i\theta_\gamma(\kappa,z)} \tag{33}$$

where θ_γ is a function of z and κ which shall be determined by requirements on the corss-spectral phase angle θ. This factorization is sufficient to guarantee that the process $v(x,z)$ possesses the autospectral density function of the process $u(x,z)$ as required.

C. Phase Angle Matching

In this section we develop the appropriate matching between the filter and the turbulence statistics phase angles (Eq.6). If we express H_γ, H_p, and ϕ_s in polar form ($\approx e^{-i\theta}$) then it follows from the previous development that

$$\theta(\kappa,\Delta,z) = \theta_\gamma(\kappa,z) - \theta_\gamma(\kappa,z-\Delta) + \theta_p(\kappa,z) - \theta_p(\kappa,z-\Delta) + \theta_s(\kappa,\Delta) \tag{34}$$

where subscripts denote the quantity involved and the various θ's are defined in the sense of Eq. (7). The quantity θ_s is given by

$$\theta_s(\kappa,\Delta) = \tan^{-1}\left[\frac{\sum_{k=1}^{n} b_k \sin\left(\frac{\kappa\Delta}{\epsilon_o}\pi(k-1)+\beta\right)}{\sum_{k=1}^{n} b_k \cos\left(\frac{\kappa\Delta}{\epsilon_o}\pi(k-1)+\beta\right)}\right] \tag{35}$$

The b's have been determined to match the coherence and the quantity θ_p is a known function of κ and z [Eqs. (31) and (32)]; however the quantity β and the function $\theta_\gamma(\kappa,z)$ can be chosen so as to satisfy the phase angle matching requirement Eq. (34).

IV. Longitudinal Gust Statistics

The spectral data required to implement the simulation scheme outlined in the previous sections consist of longitudinal auto-spectra and the coherence and phase angle associated with the interlevel longitudinal cross-spectra. In this section we shall discuss these statistics.

A. Longitudinal Auto-Spectra

Extensive data exists on the longitudinal component of turbulence. The reader is referred to review papers by Teunissen[7] Luers,[8] Busch,[9] and Fichtl[10] on the subject of longitudinal spectra which encompass contributions up to approximately the middle of 1972. A recent and particularly noteworthy contribution reported in the literature since that time is Ref. 11 which documents very detailed and precise measurements of turbulence spectra in the first 23 m of the atmosphere. All of these publications show that in a turbulent atmospheric boundary layer the longitudinal spectrum at sufficiently large values of κ asymptotically behaves like

$$\phi(\kappa,o,z) = \alpha\epsilon^{2/3}(z)\kappa^{-5/3},\ \kappa\mapsto\infty \tag{36}$$

where ϵ is the viscous dissipation rate of turbulent kinetic energy per unit mass and α is a universal constant[12] with numerical value approximately equal to 0.26. Equation (36) is the longitudinal spectrum for the inertial subrange and was first proposed by Kolmogorov.[13] Since that time it has been found to be valid for many kinds of turbulent flows ranging from laboratory scales[14] to those scales of motion in stars.[15,16] As κ decreases the longitudinal spectrum departs from that given by Eq. (36) and tends to approach a constant. Various functions have been proposed for the longitudinal spectrum which merge the low wave number region with the high wave number asymptotic behavior given in Eq. (36). In most cases the formulas are rather complicated which can result in complex simulation procedures. In addition, the low wave number region of the longitudinal spectrum does not seem to have universal behavior, but rather depends on both the near and far field terrain surrounding the meteorological site at which the spectrum is measured. Nevertheless, attempts have been made to model the longitudinal spectrum with the Monin-Obukhov-Lettau similarity hypothesis for the surface boundary layer.[9]

A longitudinal auto-spectrum which has been widely used in the aeronautical and aerospace communities and which satisfies the low and high wave number behavior discussed above is that due to von Karman[17] namely

$$\phi(\kappa,o,z) = \frac{\sigma^2(z)L(z)}{\pi}\,[1+(1.339L(z)\kappa)^2]^{-5/6} \tag{37}$$

where $\sigma(z)$ and $L(z)$ denote the standard deviation and integral scale of turbulence at height z above natural grade. The fact that this spectrum is not rational can result in turbulence simulation difficulties. A way to circumvent these problems is to approximate this spectral density function over the wave-number band of potential concern with a meromorphic function of the form[18]

$$\phi(\kappa,o,z) = \frac{b_o+b_1(L\kappa)^2+\ldots+b_m(L\kappa)^{2m}}{a_o+a_1(L\kappa)^2+\ldots+a_{m+1}(L\kappa)^{2m+2}} \tag{38}$$

where the a's and b's are functions of z. We can express Eq. (38) in the form

$$\phi(\kappa,o,z) = \frac{\sigma^2L}{\pi}\,\frac{a_o'}{a_o'+(\kappa L)^2} \times\left[\frac{1+b_1'(\kappa L)^2+\ldots+b_m'(\kappa L)^{2m}}{1+a_1'(\kappa L)^2+\ldots+a_m'(\kappa L)^{2m}}\right] \tag{39}$$

where the a''s and b''s are functions of z. At $\kappa=0$ Eqs. (37) and (39) agree exactly. As κL departs from zero, Eq. (39) will depart from Eq. (37). However, the a''s and b''s could be chosen so as to minimize the error over a band of wave number, $-\kappa_c\le\kappa\le\kappa_c$, of concern subject to the constraint

$$\int_{-\infty}^{\infty}\phi(\tau,o,z)\,d\kappa=\sigma^2 \tag{40}$$

We will not discuss this point further except to say that these techniques do exist.[18] The simplest approximate mermorphic representation of $\phi(\kappa,o,z)$ is that obtained from Eq. (39) by setting $a_o'=1$ and $a_i'=b_i'=o(i=1,2,3\ldots m)$ so that

$$\phi(\kappa,o,z) = \frac{\sigma^2L}{\pi}\,\frac{1}{1+(\kappa L)^2} \tag{41}$$

This function is the longitudinal spectral density function proposed by Dryden.[19] The quantity $a_o'=1$ results from the constraint given by Eq. (40). Equation (41) has been widely used in the aeronautical and aerospace communities for the simulation of flight in atmospheric turbulence. As $\kappa L\mapsto\infty$, Eq. (41) asymptotically behaves like

$$\phi(\kappa,o,z) = \frac{\sigma^2}{\pi L}\,\kappa^{-2},\ \kappa\mapsto\infty \tag{42}$$

Thus, the Dryden spectrum will decrease faster than the von Karman spectrum as $\kappa L\mapsto\infty$. This means the percentage error resulting in the use of Eq. (41) to represent the von Karman spectrum will increase as κL increases. This error can be reduced over a prescribed wave number band by judicious selection of values for the a's and b's in Eq. (39). In the application that follows we shall use Eq. (41) because of its simple form and more importantly because in many practical cases it provides for an adequate simulation of turbulence.

B. Standard Deviation and Integral Scale of Turbulence

To determine values of σ and L for a simulation we return to Eq. (37). In particular we will discuss the determination of σ and L for the horizontally homogeneous and statistically stationary surface boundary layer for which the Monin-Obukhov-Lettau similarity hypothesis is valid. According to Ref. 9, available meteorological data appears to suggest that $\phi(\kappa,o,z)$ can be functionally expressed as

$$\frac{\kappa\phi(\kappa,o,z)}{u_{*o}^2} = G(\kappa z, z/L_o) \tag{43}$$

where G is a universal function κz and z/L_o, u_{*o} is the surface function velocity, and L_o is the Monin-Obukhov-Lettau stability length. We now render the von Karman spectrum, Eq. (37), nondimensional in accord with Eq. (43) to obtain

$$\frac{\kappa\phi(\kappa,o,z)}{u_{*o}^2} = \frac{1}{\pi}\left(\frac{\sigma}{u_{*o}}\right)^2\left(\frac{L}{z}\right) \times\frac{\kappa z}{[1+(1.339(L/z)\kappa_z)^2]^{5/6}} \tag{44}$$

Comparison of Eqs. (43) and (44) yields

$$(\sigma/u_{*o}) = F_1(z/L_o) \tag{45}$$

and

$$(L/z) = F_2(z/L_o) \tag{46}$$

where F_1 and F_2 are universal functions of z/L_o. Upon rendering Eq. (36) nondimensional according to the scaling formula given by Eq. (43) and comparison of the resulting relationship with the asymptotic form of Eq.(44) as $\kappa z\mapsto\infty$ we determine the function $F_2(z/L_o)$, i.e.,

$$F_2(z/L_o) = \frac{k_1}{(1.339)^{5/2}(\pi\alpha)^{3/2}}\,\frac{F_1^3(z/L_o)}{\phi_\epsilon(z/L_o)} \tag{47}$$

where k_1 is von Karman's constant with numerical value approximately equal to 0.4 and ϕ_ϵ is the nondimensional viscous dissipation, namely

$$\phi_\epsilon = (k_1 z\epsilon/u_{*_o}^3) \tag{48}$$

The quantity ϕ_ϵ is a universal function of z/L_o according to the Monin-Obukhov-Lettau similarity hypothesis.[21] The functions F_1 and ϕ_ϵ are known functions of z/L_o so that σ and L are known functions of height upon specifying u_{*_o} and L_o.

This analysis can be extended to the turbulent Ekman layer by hypothesizing the existence of a universal function of the nondimensional longitudinal spectrum, functionally of the form

$$\frac{\kappa\phi(\kappa,o,z)}{u_{*_o}^2} = G(\kappa z, z/L_o, fz/u_{*_o}, z/\delta) \tag{49}$$

where f is the Coriolis parameter and δ is the boundary-layer thickness. In this particular case we are considering a barotropic Ekman layer. To extend the analysis to baroclinic boundary layers nondimensional quantities characterizing the baroclinicity of the layer are required. If the scaling law given by Eq. (49) is correct then the equations for σ and L are given by

$$(\sigma/u_{*_o}) = F_1(z/L_o, fz/u_{*_o}, z/\delta) \tag{50}$$

$$\frac{L}{z} \frac{k_1}{(1.339)^{5/2}(\pi\alpha)^{3/2}} \frac{F_1^3(z/L_o, fz/u_{*_o}, z/\delta)}{\phi_\epsilon(z/L_o, fz/u_{*_o}, z/\delta)} \tag{51}$$

The precise behaviors of the functions F_1 and ϕ_ϵ in the Ekman layer are not experimentally well known. However, in the neutral boundary layer ($z/L_o = 0$) it appears that $\delta \propto u_{*_o}/f$ (Refs. 22 and 23), so that Eqs. (50) and (51) reduce to

$$(\sigma/u_{*_o}) = F_1(fz/u_{*_o}) \tag{52}$$

$$\frac{L}{z} = \frac{k_1}{(1.339)^{5/2}(\pi\alpha)^{3/2}} \frac{F_1^3(fz/u_{*_o})}{\phi_\epsilon(fz/u_{*_o})} \tag{53}$$

Controversy exists concerning the unstable Ekman layer. One theory[24,25] states that u_{*_o}/f is irrelevant. Another theory[26] states that in addition to the parameter fz/u_{*_o} one need only introduce z/L_o to characterize heat flux effects so that nondimensional quantities like σ/u_{*_o} and L/z are universal functions of fz/u_{*_o} and z/L_o. The resolution of this controvery awaits adequate experimental data. We believe that both theories have merits and rather than discard u_{*_o}/f in favor of δ or vice versa both quantities should be incorporated into a viable boundary-layer theory. Very little is known about the stably stratified Ekman layer and future developments must await results from sufficient detailed experiments. The major problem in the stable Ekman layer is the tendency of the stable stratification to retard interlevel turbulent coupling.

Let us now return to the surface layer analysis. In the neutral ($z/L_o = 0$) surface layer the functions F_1 and ϕ_ϵ reduce to constants, namely $F_1(0) = 2.5$ (Ref. 27) $\phi_\epsilon(0) = 1$ (Ref. 28), so that

$$\sigma = 2.5u_{*_o} \tag{54a}$$

$$L = K_1 z \tag{54b}$$

where $K_1 = 4.08$. This linear dependence of L on z is in agreement with available data.[8] As z/L_o departs from zero toward instability ($z/L_o < 0$) and stability ($z/L_o > 0$) $F_1(z/L_o$ increases and decreases respectively, thus resulting in a vertical distribution of σ. In unstable and stable air the dependence of L on z will depend on the model that is selected for ϕ_ϵ. The form of ϕ_ϵ depends curcially on the turbulent energy budget.[28-30] Thus, for example, if one assumes that production and dissipation of turbulent energy are in balance, which many tower measurements seem to suggest, then it can be shown that

$$\phi_\epsilon(z/L_o) = \phi_u(z/L_o) - z/L_o \tag{55}$$

(Ref. 8) where $\phi_u = (k_1 z/u_{*_o})\partial\bar{u}/\partial z$ is the nondimensional first derivative of the mean wind speed. The quantity ϕ_u is a universal, monotonically increasing function of z/L_o with $\phi_u(o) = 1$. This model with the behavior of $F_1(z/L_o)$ given in Ref. 27 leads to the well observed result that L increases with altitude at a rate slower than z in stable air and increases with altitude at a rate faster than z in unstable air. This means that at a given altitude z as the boundary layer becomes unstable the longitudinal spectrum tends to shift toward smaller wave numbers and *vice versa* for the stable boundary layer, which are well confirmed results.[30]

C. Coherence and Phase

The interlevel longitudinal spectra or equivalently the interlevel coherence and phase angle, Eqs. (5) and (6), have only been studied until very recently so that available data are sparse in relation to the amount of data on longitudinal autospectra at a given level. The available data on longitudinal coherence and phase appear to show that in the surface layer the following scaling laws are valid

$$\mathrm{coh}(\kappa,\Delta,z) = I_1(\kappa\Delta, z/L_o) \tag{56}$$

$$S \equiv \theta(\kappa,\Delta,z/\kappa\Delta) = I_2(\kappa\Delta, z/L_o) \tag{57}$$

where I_1 and I_2 are universal functions.[31] The quantity S is called the "eddy-slope" in the meteorological literature. It appears that these laws can be extrapolated up to approximately the 100 m level. Above this level an added height dependence should be included, i.e., quantities like fz/u_{*_o} and z/δ should be included in the arguments of the functions I_1 and I_2. The scaling laws state that short eddies (large κ) over short vertical distances (small Δ) have the same coherence and phase as long eddies (small κ) over large vertical distances (large Δ).

Available experimental evidence appears to suggest that the functions I_1 and I_2 are given by[31]

$$I_1(\kappa\Delta, z/L_o) = e^{-(a/2\pi)\kappa\Delta} \tag{58}$$

$$I_2(\kappa\Delta, z/L_o) = I_3(z/L_o) \tag{59}$$

where a and I_3 are monotonically increasing functions of z/L_o with $a(0) \simeq 19$ and $I_3(0) \simeq 1$. Thus, at a given value of $\kappa\Delta$ the interlevel longitudinal coherence in unstable air is larger than the corresponding value of coherence in stable air, while the reverse is true for the "eddy-slope" S. The analysis that follows will be based on Eqs. (58) and (59).

V. Longitudinal Gust Simulation/Application

In this section we shall combine the theoretical development and empirical longitudinal gust statistics presented in the previous sections to demonstrate the practical aspects of the simulation of turbulence. In our discussion we will use the Dryden approximation to the longitudinal spectral density function, Eq. (41) with σ and L given by Eqs. (54) and the interlevel spectral coherence and phase functions given by Eqs. (56-59) for $z/L_o = 0$. The latter equations show that the interlevel spectral coherence and phase angle of the random process $v(x,z)$ should depend on $\kappa\Delta$ only. In addition, in the neutral stability case ($z/L_o = 0$) the dependence of the

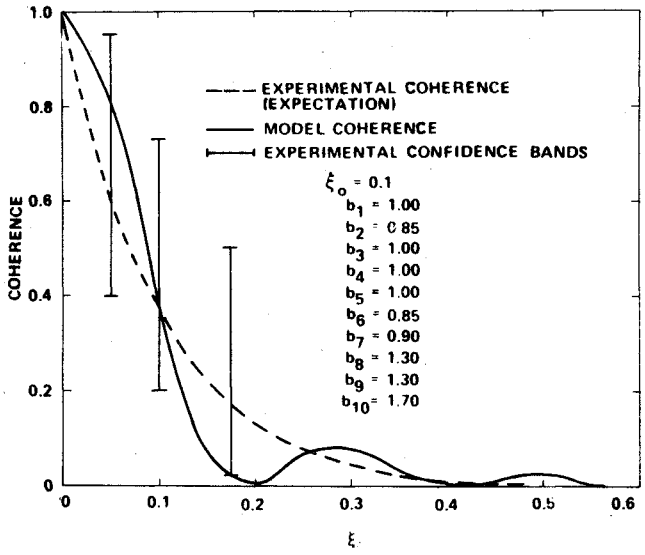

Fig. 1 Experimental and model ($\xi = 0.1$) coherence as functions of ξ.

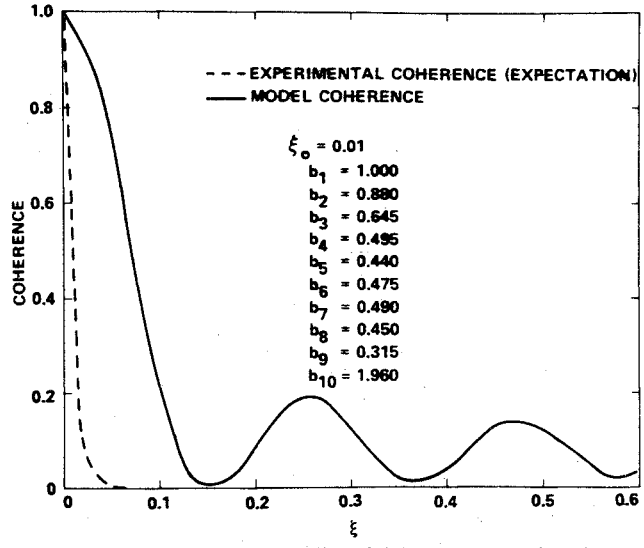

Fig. 2 Experimental and model ($\xi_o = 0.01$) coherence as functions of ξ.

coherence and phase angle on z should vanish. We shall restrict the analysis in this section to the neutral case; however, we shall allude to the stable and unstable cases in our discussion concerning self-similar properties of the filter.

A. Coherence Determination

In the neutral case it is clear that Eq. (21) satisfies the scaling law given by Eq. (56) in view of the fact that κ and Δ are present only as a product. Transformation of $\kappa\Delta$ in Eq. (58) to the dependent variable ξ [see Eq. (22)] yields

$$\mathrm{coh}(\xi) = e^{-\xi/\xi_o} \tag{60}$$

where

$$\xi = (2\pi/a\epsilon_o) \tag{61}$$

Substitution of Eq. (60) into Eq. (23) yields

$$\frac{2\xi_o(e^{\xi_o^{-1}}(-1)^{j-1}+1)}{1+(j\pi\xi_o)^2} \tag{62}$$

To estimate the parameter ξ_o in this particular example, we note that if a linear aerospace or aeronautical system travels with speed V_s through a Fourier component of turbulence with wave number κ, then a response in the system will be excited at frequency ω (rad sec^{-1}) given by

$$\omega = V_s\kappa \tag{63}$$

so that

$$\kappa\Delta = (\omega\Delta/V_s) \tag{64}$$

The quantity ϵ_o is defined as the largest value of $\kappa\Delta$ of concern which is obtained by maximizing $\omega\Delta$ and minimizing V_s. If we confine the simulation to the first 300 m of the boundary layer, then the largest value of $\Delta \sim 0(300$ m). During a simulation we are interested in the control capability of the system or pilot so that the largest value of $\omega \sim 0(2\pi$ rad sec$^{-1})$. In addition, the smallest value of $V_s \sim 0(50$ m sec$^{-1})$, so that with $a = 19$ (see Sec. 4C) the smallest value of the simulation parameter $\xi_o \sim 0(0.01)$. An upper bound on $\xi_o = \infty$, which corresponds to $a = 0$ or perfect coherence for arbitrary ξ (a physically impossible case). A physically real upper bound on ξ_o might be obtained by examining the case in which the largest permissible frequency of the system is the phugoid mode[17] which for most aircraft during take-off and landing is

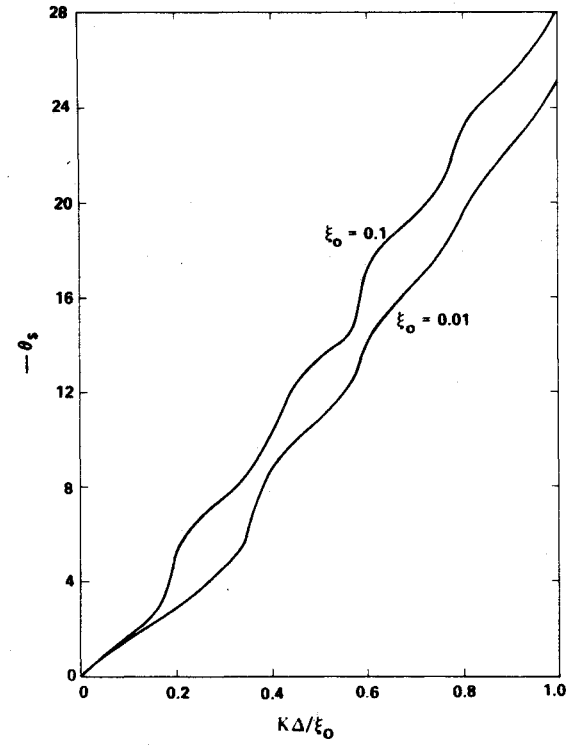

Fig. 3 The function $-\theta_s$ vs $\kappa\Delta/\epsilon_o$ for $\xi_o = 0.1$ and 0.01.

on the order of g/V_s where g is the acceleration of gravity (9.8 m sec^{-2}). Substitution of the previous values of V_s and a [see Eq. (58)] with the phugoid frequency yields an upper bound on $\xi_o \sim 0(1)$.

Figure 1 is an example of the coherence of the simulation model in which $\xi_o = 0.1$. In this particular case we used a Fourier expansion, as previously described, in which we have truncated the expansion after the tenth term. In the figure we have indicated the values of b_k ($k = 1,2,\ldots 10$) associated with the values of the A's derived from Eq. (62). We have also indicated in the figure typical 95% confidence limits of coherence data from many sites. It is apparent from the figure that a ten-term expansion results in an adequate representation for engineering applications.

Figure 2 is an example of the coherence for $\xi_o = 0.01$ where we have again used a ten-term expansion. In this particular case the simulation model fails to have coherence fidelity. To remedy this situation an increase in the number of terms

(noise sources) in the Fourier expansion of the coherence by a factor of 5 to 10 would be required.

B. Auto-Spectra Factorization

In view of Eqs. (32) and (41) the function $H_p(\kappa,z)$ in this particular example is given by

$$H_p(\kappa,z)=\sigma\left[\frac{L}{\pi}\right]^{1/2}\frac{1}{1+i\kappa L} \tag{65}$$

where $L=K_1 z$. This result will be used in the following sections to determine phase angles and for system self-similar considerations.

C. Phase Angle Determination

According to Eqs. (34) and (59), for the neutral case ($S=1$), we can write

$$\theta=\kappa\Delta=\theta_p(\kappa,z)-\theta_p(\kappa,z-\Delta)+\theta_\gamma(\kappa,z)$$
$$-\theta_\gamma(\kappa,z-\Delta)+\theta_s(\kappa\Delta) \tag{66}$$

where $\theta_s(\kappa\Delta)$ is given by Eq. (35) and is a known function of $\kappa\Delta$. The functions $\theta_s(\kappa\Delta)$ for $\zeta_o=0.1$ and 0.01 are given in Fig. 3. It is readily seen that for engineering application purposes $\theta_s(\kappa\Delta)$ can be approximated as a linear function of $\kappa\Delta$, i.e.,

$$\theta_s(\kappa\Delta)=c(n,\epsilon_o)\kappa\Delta \tag{67}$$

where $c(n,\epsilon_o)$ is a function of the noise source number, n, and the nondimensional cut-off wave number, ϵ_o. We found this linear approximation to be valid for $3\leq n\leq 10$ and $0.1<\epsilon_o\leq 0.01$.

The quantity $\theta_p(\kappa,z)$ by definition is given by

$$\theta_p(\kappa,z)=\tan^{-1}(\kappa L)=\tan^{-1}(\kappa,\kappa z) \tag{68}$$

which is derivable from Eq. (65)

Substitution of Eqs. (67) and (68) into Eq. (66) yields

$$\theta_\gamma(\kappa,z)=\kappa z(1-c)-\tan^{-1}\kappa K_1 z+G_o(\kappa,z_r) \tag{69}$$

where $G_o(\kappa,z_r)$ is an arbitrary function of κ and a reference height z_r. For definitness we shall set this function equal to zero.

VI. Self-Similar Simulation

In the previous sections we derived the appropriate response function for the simulation of the longitudinal component of turbulence in the context of a first-order Dryden auto-spectrum. The resulting mathematical system permits the simulation of the random function field $v(x,z)$. This function field is useful in many applications; however, in aeronautical and aerospace vehicle applications we desire the function

$$v(t)=v(X(t),Z(t)) \tag{70}$$

where $X(t)$ and $Z(t)$ are the horizontal and vertical coordinates of the vehicle at time t along its trajectory. A basic assumption here is that the turbulence is frozen in the flow or in other words Taylor's hypothesis is assumed to be valid. To generate the function $v(t)$ we thus evaluate $v(x,z)$ along the trajectory of the vehicle. This could be impractical in the sense that the entire random function field is needed to determine the function $v(t)$. However, in the present analysis we can circumvent these problems by appealing to the self-similar properties of the model under discussion.

A. Inverse Fourier Transformation

Combination of Eqs. (9, 17, 31, 65, and 70) yields the result

$$\frac{\hat{v}(\kappa,z)}{\sigma(z)L^{1/2}(z)}=\left[\pi\sum_{k=1}^{n}b_k\right]^{-1/2}(1+(\kappa L)^2)^{-1/2}$$
$$\times\sum_{k=1}^{n}b_k^{1/2}e^{-i\kappa z(1+d_k-c)}\hat{N}_k(\kappa) \tag{71}$$

where $L(z)=K_1 z$. This statement can be transformed into (x,z)-space to yield

$$\frac{v(x,z)}{\sigma(z)L^{1/2}(z)}=\left[\pi\sum_{k=1}^{n}b_k\right]^{1/2}$$
$$\times\sum_{k=1}^{n}b_k P_k(x-z(1-b_k-c)) \tag{72}$$

where

$$P_k(\xi)=\frac{1}{2\pi}\int_{-\infty}^{\infty}\frac{\hat{N}_k(\kappa)}{(1+(K_1 z\kappa)^2)^{1/2}}e^{i\kappa\xi}d\kappa \tag{73}$$

or

$$P_k(\xi)=\frac{1}{K_1\pi z}\int_{-\infty}^{\infty}K_o\left[\frac{|\xi'|}{zK_1}\right]N_k(\xi-\xi')d\xi' \tag{74}$$

where K_o is the zero-order modified Bessel function of the second kind. Let us now map the noise process $N_k(x)$ from the x-domain to the x/z-domain and denote this mapping by $M_k(x/z)$ which is still a Gaussian, white noise process with unit spectral density. This transformation permits us to express Eq. (72) with the form

$$\frac{v(x,z)}{\sigma(z)L^{1/2}(z)}=\left[\pi\sum_{k=1}^{n}b_k\right]^{-1/2}$$
$$\times\sum_{k=1}^{n}b_k P_k'\left[\frac{x}{z}-(1+b_k-c)\right] \tag{75}$$

where P_k' is a "universal" function of x/z and is given by

$$P_k'\left(\frac{x}{z}\right)=\frac{1}{K_1\pi}\int_{-\infty}^{\infty}K_o\left[\frac{|\zeta'|}{K_1}\right]\times M_k\left[\frac{x}{z}-\zeta'\right]d\zeta' \tag{76}$$

Thus by generating a white noise process $M_k(\zeta)$, convolving it according to Eq. (76), then lagging it in x/z-space by a distance $(1+b_k-c)$, and finally summing over the n noise processes according to Eq. (75) yields a "universal" random function $F(x/z)$ for the random variable $v(x,z)/\sigma(z)L^{1/2}(z)$. In short we have transformed the random function field $v(x,z)$ of two independent variables to a random function process $F(x/z)$ with one independent variable and in this sense we speak of $F(x/z)$ being a self-similar simulation of the wind process $u(x,z)/\sigma(z)L^{1/2}(z)$.

B. Transformation to Vehicle Time Domain

As noted earlier, to determine the process $v(t)$ [Eq. (70)] along the trajectory of an aeronautical or aerospace vehicle we merely evaluate Eq. (75) at the location of the vehicle $[(X(t), Z(t)]$. This yields

$$\frac{v(t)}{\sigma(Z(t))L^{1/2}(Z(t))}=\left[\pi\sum_{k=1}^{n}b_k\right]^{-1/2}$$
$$\times\sum_{k=1}^{n}b_k P_k'\left[\frac{X(t)}{Z(t)}-(1+b_k-c)\right] \tag{77}$$

Thus it is possible to perform a simulation of atmospheric turbulence which retains the nonstationary character of turbulence relative to a vehicle ascending or descending in the atmospheric boundary layer for the trajectory only and thus avoid explicit evaluation of the entire two-dimensional velocity field.

C. Self-Similar Simulation/A Second Look

The self-similar solution rests upon the integral scale being a linear function of height. Thus, in unstable and stable boundary layers in which the vertical dependence of L departs markedly from a linear behavior a self-similar simulation like that previously discussed may not be available. In addition, Monin-Obukhov length effects would then become important which, if in fact a self-similar simulation did exist, then it would at best only allow for a "universal" representation of $v(x,z)/\sigma(z)L^{1/3}(z)$ functionally of the form $F(x/z,\ z/L_o)$. In other words, if a self-similar simulation did exist for stable and unstable flows it would not be one-dimensional as in the neutral case because of the presence of the independent variable z/L_o.

A second point which should be noted is that the functional form of $\sigma(z)$ does not play a critical role in the self-similar theory because $\sigma(z)$ only enters the theory via a division of $v(x,z)$. In the special case of the neutral surface layer $\sigma=$ constant. However, this requirement can be used with an integral scale which depends linearly on height because the linear dependence of L on z in the neutral case extends to greater heights ($z \lesssim 200$ m) than the attendant height invariant behavior of σ in the neutral surface layer. This then permits self-similar turbulent simulation in neutral boundary layers up to approximately the 200-meter level.

VII. Epilogue

The concepts of nonstationary turbulence simulation, especially the self-similar aspects of the subject, represent what we believe to be a viable new approach to the solution of a long outstanding problem. Although the development was restricted to atmospheric turbulent random process fields we believe that the technique is sufficiently general so as to be applicable to other two-dimensional random function fields. In these other applications the self-similar properties may not be available; however, the mathematical machinery prior to the self-similar developments herein should be applicable.

The technique developed herein is a practical one and the implementation of the model should be no more difficult than currently available procedures which are capable of simulating a process which only satisfies the auto-spectra properties of atmospheric turbulence.

The analysis serves to indicate areas of deficiencies relative to the observational aspects of atmospheric turbulence. Improvements in the fidelity of the model can only be accomplished through better empirical definition of the auto-spectra, coherence, and phase angle θ. Of the three ingredients to the model the latter two require further study.

An important point in the analysis was the factorization of the auto-spectra and thus the occurrence of the phase angle $\theta_\gamma(\kappa,z)$ [see Eq. (69)] permitted the interlevel phase angle θ to be satisfied. The question that must be answered concerns whether or not $\theta_\gamma(\kappa,z)$ as modeled herein is valid. The phase angle $\theta_p+\theta_\gamma$ plays a crucial role in the theory of intermittent turbulence[32] because it is only through these phase angles that occassional large gusts can occur. From the development in Sec. V,

$$\theta_p+\theta_\gamma=\kappa z(1-c) \tag{78}$$

Differences between this result and experiment will occur because we have replaced the Kolmogorov inertial subrange in the von Karman spectrum [Eq. (37)] with a first-order meromorphic representation (Dryden form). However, these differences we believe to be minor and within the expected experimental range of variation. If Eq. (69) departs significantly from experiment it will be due primarily to the function θ_γ selected to satisfy the interlevel phase angle requirements. In our analysis we set $G_o(\kappa,z_r)=0$ [see Eq. (69)]. If it should turn out that Eq. (69) is not valid then a nonzero function $G_o(\kappa,z_r)$ might be selected to satisfy the experimental results. This may not be possible because a z-dependence in the function $G_o(\kappa,r_r)$ is not available. In addition, the inclusion of a nonzero function for $G_o(\kappa,r_r)$ would destroy the self-similar properties of the model because of the appearance of the non-dimensional ratio z/z_r in the argument of the function $F(x/z)$.

References

[1] Wright, O., "How We Made the First Flight," *Flying*, Dec. 1913, pp. 10-12, 35-36.

[2] "Flight in Turbulence Advisory Group for Aerospace Research and Development," AGARD Conference Proceedings No. 140, Neuilly Sur Seine, France, 1973.

[3] Saldana, R., personal communication, 1974, NASA-Johnson Space Center, Houston, Texas.

[4] Reeves, P.M., "A Non-Gaussian Turbulence Simulation," AFFDL-TR-69-67, 1969, Air Force Flight Dynamics Lab., Wright-Patterson Air Force Base, Ohio.

[5] Daniels, G.E., ed., "Terrestrial Environmental (Climatic) Criteria Guidelines for Use in Space Shuttle Vehicle Development," TM X-64757, 1971 (1973 revision), NASA Marshall Space Flight Center, Huntsville, Ala.

[6] Lumley, J. L. and Panofsky, H. A., *The Structure of Atmospheric Turbulence*, Interscience, New York, 1964.

[7] Teunissen, H. W., "Characteristics of the Mean Wind and Turbulence in the Planetary Boundary Layer," UTIAS Review No. 32, 1970, University of Toronto Institute for Aerospace Studies, Toronto, Canada.

[8] Luers, J. K., "A Model of Wind Shear and Turbulence in the Surface Boundary Layer," CR-2288, 1973, NASA.

[9] Busch, N. E., "The Surface Boundary Layer," *Boundary-Layer Meteorology*, Vol. 4, 1973, pp. 213-240.

[10] Fichtl, G. H., "Problems in the Simulation of Atmospheric Boundary-Layer Flows," *AGARD Conference Proceedings No. 140*, Advisory Group for Aerospace R&D, Neuilly Sur Seine, France, 1973.

[11] Kaimal, J.C., Wyngaard, J. C., and Izumi, Y., "Spectral Characteristics of Surface-Layer Turbulence, *"Quarterly Journal, Royal Meteorological Society*, Vol. 98, Feb. 1972, pp. 563-589.

[12] Paquin, J. E. and Pond, S., "The Determination of the Kolmogoroff Constants for Velocity, Temperature, and Humidity Fluctuations from Second- and Third-Order Structure Functions," *The Journal of Fluid Mechanics*, Vol. 50, 1971, pp. 257-269.

[13] Kolmogoroff, A. N., "The Local Structure of Turbulence in Incompressible Viscous Fluid for Very Large Reynolds Numbers,"*Doklady Akademii Nauk SSSR*, Vol. 30, 1941, pp. 301-305.

[14] Hinze, J. O., *Turbulence, An Introduction to its Mechanism and Theory*, McGraw-Hill, New York, 1959.

[15] Nakagawa, Y. and Priest, E. R., "A Possible New Interpretation of Power Spectra of Solar-Granulation Brightness Fluctuations," *The Astrophysical Journal*, Vol. 178, June 1972, pp. 251-255.

[16] Silk, J. and Ames, S., "Primordial Turbulence and the Formation of Galaxies," *The Astrophysical Journal*, Vol. 178, May 1972, pp. 77-93.

[17] Etkin, B., *Dynamics of Atmospheric Flight*, Wiley, New York, 1972.

[18] Solodovnikov, V. V., *Introduction to the Statistical Dynamics of Automatic Control Systems*, Dover, New York, 1960.

[19] Chalk, C. R., et al, "Background Information and User Guide for MIL-F-8785B (ASG), 'Military Specification—Flying Qualities of Piloted Airplanes,' " AFFDL-TR-69-72, 1969, Air Force Flight Dynamics Lab., Wright-Patterson Air Force Base, Ohio.

[20] Panofsky, H. A., "The Boundary Layer about 30 Meters," *Boundary-Layer Meteorology*, Vol. 4, Sept. 1973, pp. 251-264.

[21] Monin, A. S. and Yaglom, A. M., *Statistical Fluid Mechanics: Mechanics of Turbulence; Vol. 1*, MIT Press, Cambridge, Mass., 1971.

[22] Blackadar, A. K. and Tennekes, H., "Asymptotic Similarity in Neutral Barotropic Planetary Boundary Layers," *Journal of the Atmospheric Sciences*, Vol. 25, Nov. 1968, pp. 1050-1120.

[23] Csanady, G. T., "On the 'Resistance Law' of a Turbulent Ekman Layer," *Journal of the Atmospheric Sciences,* Vol. 24, Sept. 1967, pp. 467-471.

[24] Deardoff, J. W., "Numerical Investigation of Neutral and Unstable Planetary Boundary Layers," *Journal of the Atmospheric Sciences* Vol. 29, Jan. 1972, pp. 91-115.

[25] Deardoff, J. W., "Preliminary Results from Numerical Integrations of the Unstable Planetary Boundary Layer," *Journal of the Atmospheric Sciences,* Vol. 27, Nov. 1970, pp. 1209-1211,

[26] Blackadar, A. K., et al, "Investigation of the Turbulent Wind Field Below 150 M Altitude at the Eastern Test Range," CR-1410, 1969, NASA.

[27] Panofsky, H. A., et al., "Properties of Wind and Temperature at Round Hill, South Dartmouth, Mass.," ECOM-0035-F, U.S. Army Electronics Command, Atmospheric Sciences Lab., Research Div., 1967, Fort Huachuca, Ariz.

[28] Fichtl, G. H. and McVehil, G. E., "Longitudinal and Lateral Spectra of Turbulence in the Atmospheric Boundary Layer at the Kennedy Space Center," *Journal of Applied Meteorology,* Vol. 9, Feb. 1970, pp. 51-63.

[29] Wyngaard, J. C. and Cote, O. R., "The Budgets of Turbulent Kinetic Energy and Temperature Variance in the Atmospheric Surface Layer," *Journal of the Atmospheric Sciences,* Vol. 28, March 1971, pp. 190-201.

[30] Busch, N.E. and Panofsky, H.A., "Recent Spectra of Atmospheric Turbulence," *Quarterly Journal of the Royal Meteorological Society,* Vol. 94, Jan. 1968, pp. 132-148.

[31] Dutton, J. A., et al, "Statistical Properties of Turbulence at the Kennedy Space Center for Aerospace Vehicle Design," CR-1889, 1971, NASA.

[32] Spark, E. H. and Dutton, J. A., "Phase Angle Considerations in the Modeling of Intermittent Turbulence," *Journal of the Atmospheric Sciences,* Vol 29, March 1972, pp. 300-303.